

Preliminary Study of Characterization of Nanoparticles from Coconut Shell as Filler Agent in Composites Materials

A.Sulaeman, Faculty of Mathematics and Natural Sciences , Institut Teknologi Bandung, Jalan Ganesha 10, Bandung 40132, Indonesia, Email: aminudin.sulaeman@gmail.com
Rudi Dungani, School of Life Sciences and Technology, Institut Teknologi Bandung, Jalan Ganesha 10, Bandung 40132, Indonesia, Email: rudi@sith.itb.ac.id
Md. Nazrul Islam, School of Life Science, Khulna University, Khulna - 9208, Bangladesh, Email: nazrul17@yahoo.com
H.P.S. Abdul Khalil, School of Industrial Technology, Universiti Sains Malaysia, Penang, Malaysia, Email: akhalilhps@usm.my
Ihak Sumaradi, School of Life Sciences and Technology, Institut Teknologi Bandung, Jalan Ganesha 10, Bandung 40132, Indonesia, Email: ihak@sith.itb.ac.id
Dede Hermawan, Faculty of Forestry, Bogor Agricultural University, Dramaga-Bogor, Indonesia, Email: dedemjmr@yahoo.com
Anne Hadiyane, School of Life Sciences and Technology, Institut Teknologi Bandung, Jalan Ganesha 10, Bandung 40132, Indonesia, Email: anne@sith.itb.ac.id

Abstract- Agricultural wastes which include shell of coconut dry fruits (CS) can be used to prepare filler in polymer composite for commercial use. The raw CS was converted into nanoparticle in 4 steps, namely, grinding, refining, sieving and high energy ball mill. The CSNs was extracted by n-hexane for oil removal process. The presence of the oil was studied by Transmission Electron Microscopy (TEM) and Energy Dispersive X-ray analysis (EDX) to identify the existence of the oil within the nanoparticle. The decomposition temperature of the nanoparticle was studied by thermal gravimetric analysis (TGA). The nanoparticle size obtained from TEM, X-ray Diffraction (XRD) analysis and particle size analyzer was found to be 10-30 nm, 21.61- 44.46 nm and 50.75-91.28 nm (with nano size distribution intensity of 75.30%) respectively. The nanoparticle CS exhibits lower degree of crystallinity, or higher of amorphous area. The nanoparticle CS shape and surface was found to be smaller with angular, irregular and crushed shapes after been ball milling process.

I. INTRODUCTION

The polymer could be enhanced of properties and at the same time reduce costs of their composites with addition fillers. There are many type filler of inorganic have been used for their purpose [1]. Currently, polymer nanocomposites is advocated to enhance polymer properties through incorporation of nanoparticles or fillers in the nanometre scale into the polymer matrices. Nanoparticles embedded in polymer matrix have increasing mechanical, physical, thermal and electrical properties compared to neat polymers [2]. Results showed an improvement the mechanical and barrier properties use nanocomposites as epoxy [3]. Thiagarajan et al. [4] found that mechanical properties were increased for composites made with the addition of nanofiller from nanoclay. Kadhim *et al.* [5] also reported an increase in mechanical properties and fracture toughness for epoxy nanocomposites reinforced with nanofiller of aluminium oxide (Al₂O₃). Futhermore, Marcincin et al. [6] reported that nanofillers in the matrix of oriented polypropylene composite increase barrier properties of UV.

Recently, plenty of wastes is produced due to the increased activity in the modern agricultural sector, include shell of coconut dry fruits. Annually, approximately 33 billion coconuts are harvested worldwide with only 15% of these coconuts being utilized for fibers and chips [7]. Coconut shell (CS) is an abundant agricultural solid waste in several of countries like Indonesia, Malaysia and Thailand. This bio agricultural waste shell which the source of siliceous material is produced after the extracted to be coconut oil in the coconut oil mill. The coconut shell is a lignocellulosics materials has application potentials in various composites [8]. However, utilization of

CS through intensified use still not optimally caused it has low economic value, whereas they can play an important supplementary role, especially in the form of particles.

Many studies showed that CS waste is one the important sources of alternative material for the furnishing materials [6], adsorbent for the removal of gases [9], activated carbon [10], and lightweight aggregate [11]. To evaluate of characterization various CS properties, many studies have been done with dimensionals in the micrometer range. There is limited information available about the characterization of CS in the nanometer range, to date, however, not much effort has been done on the utilization of CS as filler in polymer matrix. According to the literature, the natural structure of CS is excellent and low ash content [12, 13]. Furthermore, application of nanotechnology can creating, manipulating, and exploring CS as nano-structured material to produce CS nanofiller.

The objective of this paper was to analyze and characterized from properties of CS nanoparticles. The CS nanoparticles is to be used as the nanofiller (reinforcement) for enhance the properties of composites. Materials and Methods.

II. MATERIALS AND METHODS

A. Materials

Coconut shell (CS) was collected from a coconut-oil processing mill in Ciarnis, Indonesia, in the form of chips. The solvent of n-hexane was used extraction to remove oil in CS nanoparticles. The n-hexane collected from the Pentarona Chemical Company, Indonesia.

B. Methods

Preparation of CS nanoparticles: The CS were ground using a grinder/refiner to produce powder, and the powder was dried to a total evaporable moisture content of 1.5%. Nanoparticles were prepared from these CS chips by high-energy ball milling (Pulverisette, Fritsch, Germany) for 30 h with a rotation speed of 170 rpm. The milling chamber was made of tungsten carbide, and the balls were stainless steel with diameters of 19 mm, 12.7 mm, and 9.5 mm, respectively. Toluene was used to avoid agglomeration, as reported by Paul et al. [14].

Extraction and oil removal treatment: Coconut shell nanoparticles (CSNs) were dried in an oven at 105°C for 2 h to remove moisture and was cooled in desiccators before transferred into thimbles. The process was done at 75°C for 90 min as were reported by Ferreira-Dias et al. [15]. The samples from the thimble were then dried in an oven at 105°C until dried completely (moisture content to about 1.50%), and subsequently cooled in a desiccators.

Characterization the size and morphology of CSNs:

- 1) *The Particle analyzer analysis:* measurements of particle size distribution of CSNs were assessed on a MALVERN Zetasizer Ver. 6.11 (MAL 1029406, Germany) by dynamic light scattering measurements by means of a 532nm laser. The measurement of the average particle size was automatically repeated for three times based on the equipment internal setting.
- 2) *Transmission Electron Microscopy (TEM) analysis:* the CSNs were prepared in n-hexane and dispersed with an ultrasonicator for ten minutes. The samples for TEM (PHILIPS CM12, Germany) analysis were obtained by plancing a drop of the colloidal dispersion containing samples onto a carbon-coated copper grids and allowing it to dry at room temperature before being examined under the TEM.
- 3) *X-Ray Diffraction (XRD) analysis:* the XRD measurements were carried out with the help of a PHILIPS PW 1050 X-pert Diffractometer, Germany using CuK α radiation ($K\alpha = 1.54 \text{ \AA}$) with the accelerating voltage

of 40 kV and a current of 25 mA. The samples were scanned in the range from 5 to 90° of 2θ with a step size of 0.05°. From the diffractograms the particle size were obtained. From the broadening of the peak the average crystallite size was determined with the Scherrer's equation [16]:

$$D = \kappa\lambda/\beta \cos \theta \quad (1)$$

where, κ is a constant is taken as unity, λ wavelength of the radiation is full width half maximum (FWHM) in radiance of XRD peak obtained at 2θ and D is the crystallite size in nm.

4) *Scanning Electron Microscope (SEM) analysis:* SEM was used to characterize the morphology of the particles. Small portions of samples were taken and coated with gold with an ion sputter coater (Polaron SC515, Fisons Instruments, UK). A LEO Supra 50 Vp, Field Emission SEM, Carl-Zeiss SMT, Oberkochen, Germany was used for particle surface as well as surface texture analysis.

The elemental composition of CS nanoparticles: the SEM analysis was extended to obtain the elemental composition of the nanoparticles material from CSNs by means of energy dispersive X-ray (SEM-EDX) analysis. Small portions of nanoparticles material were taken and coated with gold by an ion sputter coater (Polaron SC 515, Fisons Instruments, UK). A Leo Supra 50 VP Filed Emission Scanning Electron Microscope, Zeiss EVO 50, Oberkochen, Germany was used for microscopic study.

The functional groups of CS nanoparticles: Fourier Transform Infrared Spectroscopy (FT-IR), Nicolet Avatar 360 (USA), was used to examine the functional groups. Perkin Elmer spectrum 1000 was used to obtain the spectra of each sample where 0.5 grams of sample was mixed with KBr (sample/KBr ratio 1/100). They were then pressed into transparent thin pellets. Spectral output was recorded in the transmittance mode as a function of wave number.

Thermal Analysis: thermal analyses were carried out according to Yang *et al.* [17]. The pyrolysis of CSNs was conducted in a thermogravimetric analyzer (model TGA 2050, USA). A mass of 25 mg with the flow rate 40 mL/min was heated from room temperature to 105°C under nitrogen atmosphere. Then the temperature increased rapidly to 950°C and held for 7 min under N₂ purging.

III. RESULTS AND DISCUSSION

A. Characterization of CS nanoparticle

Particle size distribution measurements by particle analyzer: The particle size distribution of CSNs are shown in Figure 1. It shows that the particle size distribution of CSNs by intensity covers wide range of particles with symmetric behavior of curve. As depicted in Fig. 1 shows also that, the diameter of the major portion of the particle ranged between 50.75 nm to 91.28 nm which covers 95.70% of the nanoparticles. Thus, the result confirms that the CS particles are in nano-structured material as were defined by Koo, [18]. From Fig. 1 is also follows that it might be impossible to obtain a perfect approximation of the uptake curves for CSNs from the uptake curve calculated for average particle diameter.

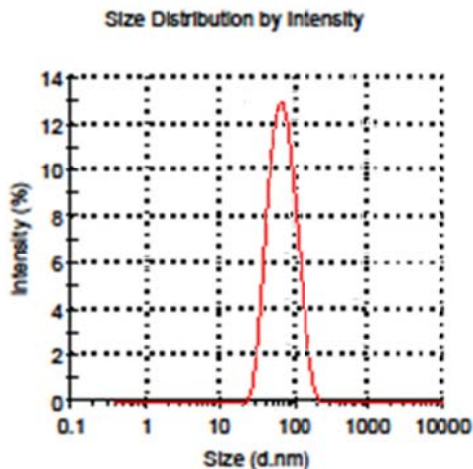


Figure 1. Particle size distribution of CSNs by intensity

Particle size measurements by TEM: the particles with different shapes and dimensions were observed by means of TEM techniques. Results from TEM shown the sample of CSNs after n-hexane extraction has relatively broad particle size distribution. The micrographs revealed that CSNs particle size ranged 10 to 50 nm (mean value of the particle size is about 50 nm). The presence of bigger formations was confirmed by transmission electron microscopy (Fig. 2).

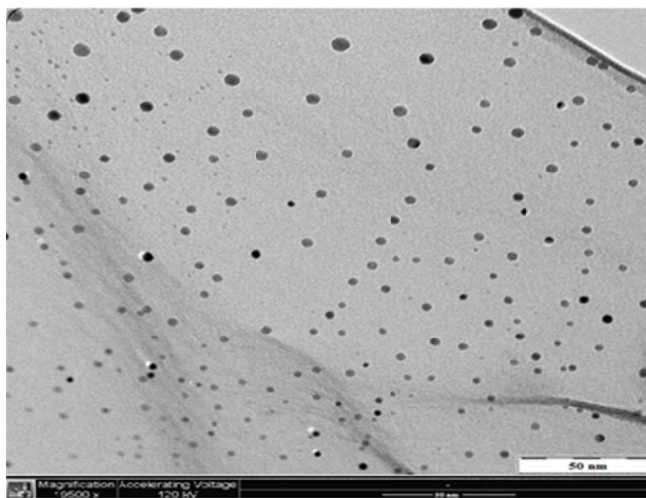


Figure 2. TEM photo of CSNs after n-hexane extraction

Particle size and crystallinity index by XRD analysis: Typical results of the XRD spectra of the CSNs samples are shown in Figure 3 and 4. As shown in Fig. 3, the XRD diffraction pattern of CSNs samples showed three strongest peak intensity at the diffraction angle 2θ which were at 20.31° , 21.15° , and 22.15° , while the low intensity peaks can be assigned to other elements present in the CSNs. Further, the average particle size was determined from X-ray diffraction peaks using the Debye-Scherrer formula (eq. 1). The reflecting peaks at $2\theta = 20.31^\circ$, 21.15° , and 22.15° were calculated to be 44.46 nm, 29.19 nm, and 21.61 nm, respectively. Thus, the average size of CSNs was calculated to be 31.75 nm.

Particle size and crystallinity index by XRD analysis: typical results of the XRD spectra of the CSNs samples are shown in Fig. 3 and 4. As shown in Fig. 3, the XRD diffraction pattern of CSNs samples showed three strongest peak intensity at the diffraction angle 2θ which were at 20.31° , 21.15° , and 22.15° , while the low intensity peaks can be assigned to other elements present in the CSNs. Further, the average particle size was determined from X-ray diffraction peaks using the Debye-Scherrer formula (eq. 1). The reflecting peaks at $2\theta = 20.31^\circ$, 21.15° , and 22.15° were calculated to be 44.46 nm, 29.19 nm, and 21.61 nm, respectively. Thus, the average size of CSNs was calculated to be 31.75 nm.

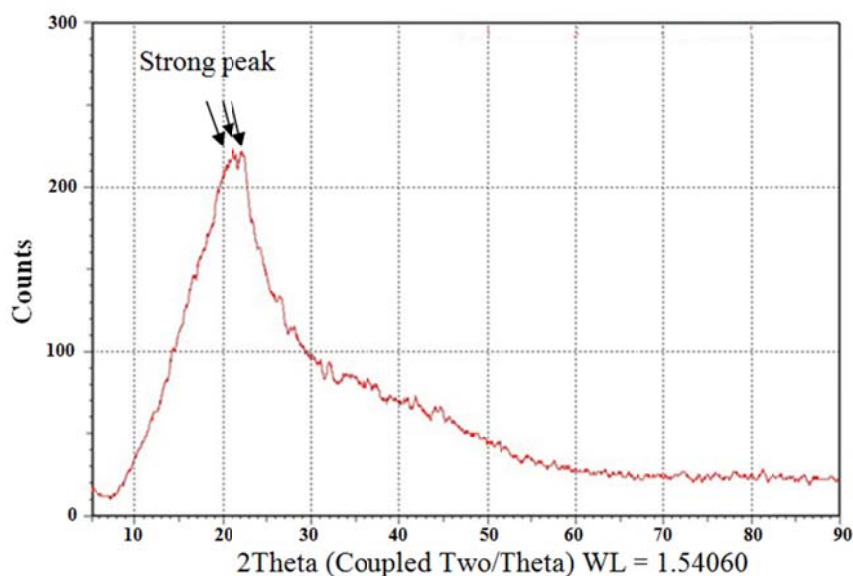


Figure 3. XRD diffraction patterns of CSNs

The crystallinity index (CI) of CSNs was calculated from XRD intensity data using peak deconvolution method. The XRD spectroscopic results in Fig. 4 were deconvulated to obtain the crystallinity index.

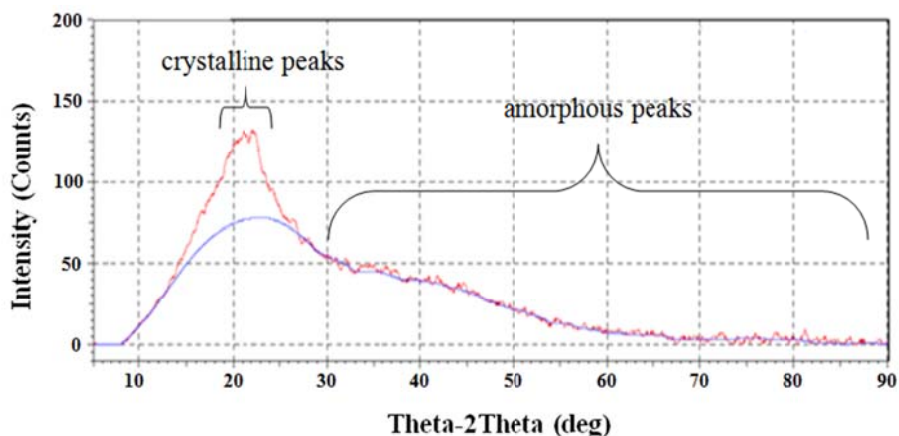


Figure 4. XRD pattern of crystalline and amorphous CSNs ranging from 2θ (5° - 90°)

There were no crystalline transformation in the structures of the samples, but there were different crystallinity levels. CSNs exhibited lower degree of crystallinity, as evidenced by number of crystalline peaks in the diffractogram. An amorphous hump was observed between 30° - 90° ; this may be due to the presence of amorphous glassy material [19]. The crystallinity indices of the nanoparticle CS were found to be equal to

15.23%. Study by XRD shown the crystallinity of nanoparticle CS decreased as the particle size decreased (Fig. 4). This result consistent with the result reported by Park et al. [19], which found that high energy ball milling decrease the size of particle together with crystallinity of the nanoparticle. Futhermore, Park et al. [19] reported that the index of crystallinity of nanofiller has a big influence in their biocomposites, such as hardness, transparency, diffusion and density.

Surface morphologies by SEM: scanning electron microscope (SEM) was used to take pictures of the powder materials to determine the general look of particles such as shape. The morphological investigation of CSNs obtained at different magnification given in Fig. 5. SEM micrograph revealed that CSNs became angular, irregular and crushed shapes. However, the raw CSNs was highly porous and sufficiently high solid densities [20]. Due to ball milling, the spherical structure of CS broke down and the particle size reduced to nanoscale with time [14]. Because of the structure of the CSNs, it is suitable for filler materials in composites [21]. Along with the solid spheres, irregular shaped particle of carbon can be seen which is larger in size. Agglomerated spheres and irregularly shaped amorphous particle can also be detected which may be because of the inter-particle fusion. However, it was not possible to detect a single particle even at higher magnifications using SEM analysis which might be related to the agglomeration of the particles and restricted of SEM analysis itself.

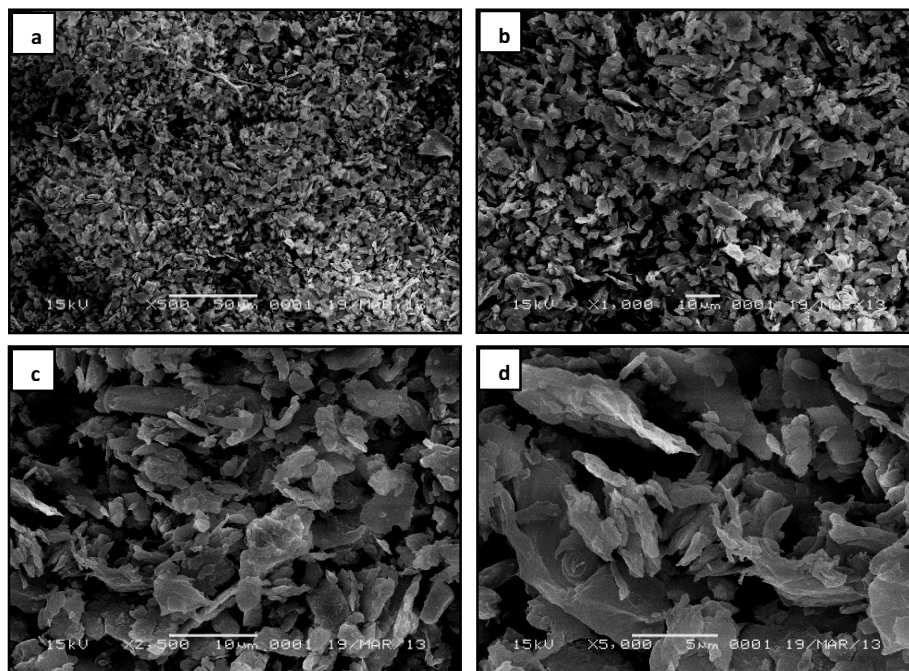


Figure 5. The SEM photomicrographs of CSNs. (a) 500x magnification; (b) 1000x magnification; (c) 2500x magnification; (d) 5000x magnification

B. Elemental composition analysis

The CSNs showed the presence of carbon, oxygen, sodium, chlorine and indium with 43.69 wt. %, 53.43 wt. %, 0.89 wt. %, 0.56 wt. %, and 1.437wt. %, respectively. This, to a great extent, is in agreement with investigation reported by Daud and Ali [22] for raw CS which showed the presence of carbon, and oxygen with 50.01 wt. % and 41.15 wt. %. According Reddy et al.[23], the presence of carbon and oxygen in the raw CS was 63.02 wt. % and 36.04 wt.%, respectively. Although, the major elements present were quite similar, the

differences observed in the elemental composition could be attributed to the particle size, and particle fabrication method [24].

Silica or silicon dioxide (SiO_2) is perhaps the most essential substance found in the CS. However, this interpretation was demonstrated by the EDX spectroscopy in Figure 5, where silica was not found at almost all major peak in the CSNs. The CSNs produced less density than silica and this showed that silica had more high mass compared with CSNs [25], thus, allegedly silica left in the bottom of the ball milling during the screening process

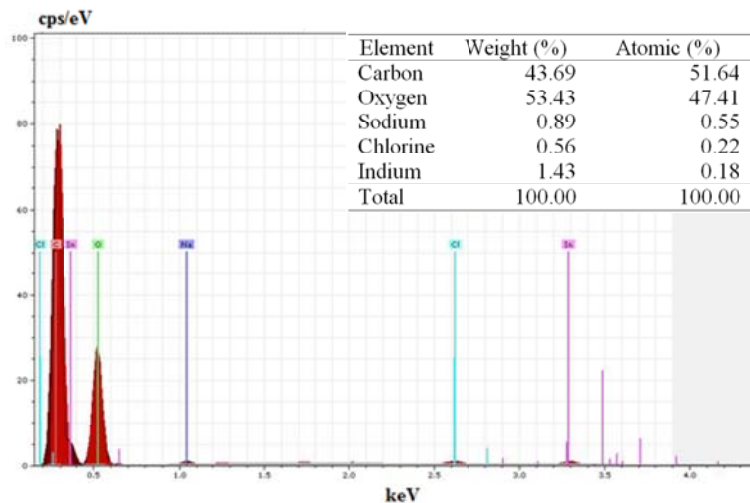


Figure 5. EDX spectrum and elemental composition of CSNs

C. Fourier transform infrared (FT-IR) Analysis

The main surface functional groups present in the CSNs were combination hydroxyl (OH), methylene groups (C-H) carbonyl groups (C=O), and ethers (C-O-C). The study by Guo and Lua, [21] in the raw CS showed that the main surface function groups presented carbonyl groups (such as ketone and quinone), ethers and phenols. This was probably due to the change of particle size during ball milling process. During the ball milling process, as the activation temperature increased, the sample lost weight was significantly due to a combination of release of volatile matters [14, 21]. The results of the FT-IR study given in Fig. 6.

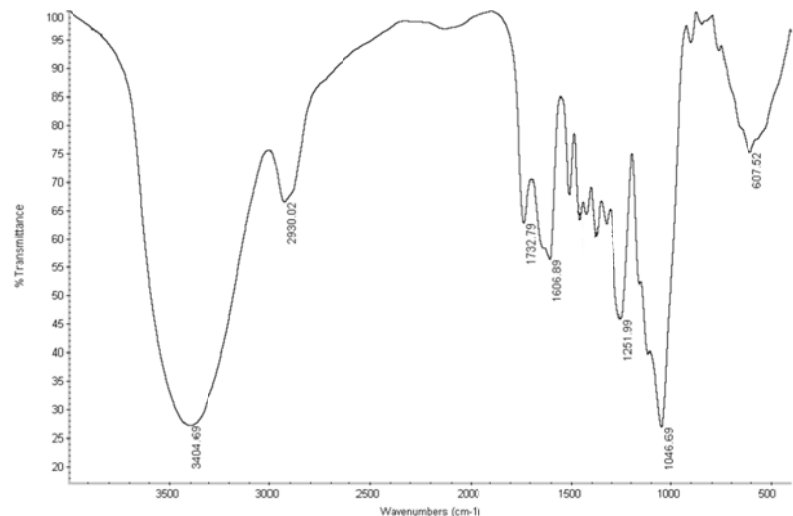


Figure 6. FT-IR spectra of CSNs

D. Thermal analysis

The TGA curves of the CSNs shown that they started to degrade at $\sim 220^{\circ}\text{C}$ and the weight loss started promptly after the temperature. When the temperature ranged between 350°C to 550°C , no obvious weight loss was observed. Above the main degradation stage, all the volatile materials were driven off from the sample resulting in the residual char or ash content about 27.73%. The main degradation of the CSNs occurred at 550°C until 850°C which showed that CSNs had more thermal stability compared with raw CS. Yang et al. [17] reported that, the particle size in the range of $250\ \mu\text{m}$ to $>2\ \text{mm}$, CS had main degradation temperature between 220°C until 340°C . The high degradation temperature of nanoparticle were due to chemical composition and the particle size in the nanometer had significant influence on pyrolysis.

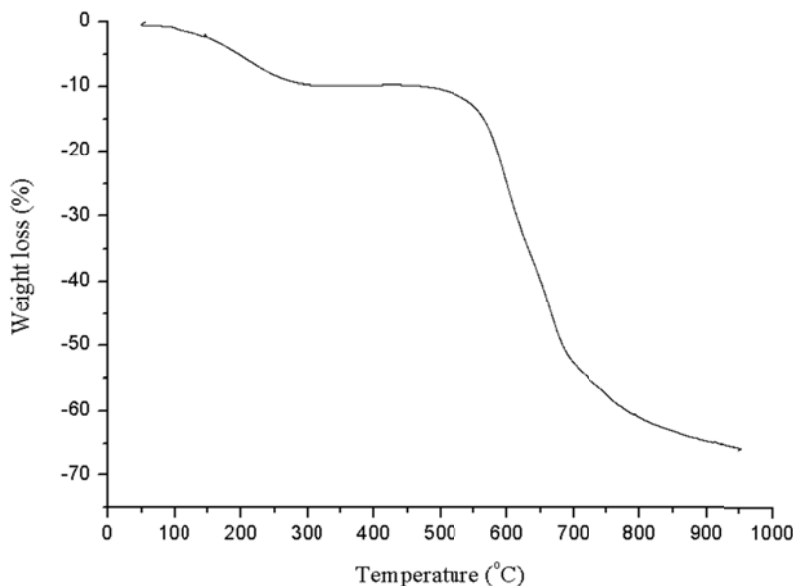


Figure 7. Thermogravimetric analysis of CSNs

IV. CONCLUSIONS

Using natural filler such as CS to reinforce the composite materials offers the following benefit in comparison with mineral filler, strong and rigid, light weight, environmental friendly, economical, renewable, and abundant resource. However, they have the disadvantage of degradation by moisture, poor surface adhesion to hydrophobic polymers, non-uniform filler sizes.

ACKNOWLEDGMENTS

The authors thank the Universiti Sains Malaysia (USM) for the awarded Postdoctoral Fellowship. The authors also extend thanks to the research collaboration between School of Industrial Technology, USM, Malaysia and School of Life Sciences and Technology, Institut Teknologi Bandung, Indonesia.

REFERENCES

- [1] L.A. Utracki, M. Sepehr, and E. Boccaleri, "Synthetic layered nanoparticles for polymeric nanocomposites (PNCs); A review," *J. Polym. Advan. Technol.*, vol. 18, no. 1, pp. 1-37, Jan. 2007.
- [2] Md. S. Islam, R. Masoodi, and H. Rostami, "The effect of nanoparticles percentage on mechanical behavior of silica-epoxy nanocomposites," *J. Nanoeurosc.*, vol. 2013, pp. 1-10, Nov. 2013.

- [3] H. Alamri, and I.M. Low, "Effect of water absorption on the mechanical properties of nanoclay filled recycled cellulose fibre reinforced epoxy hybrid nanocomposites," *Composites Part A.*, vol. 44, no. 1, pp. 23-31, Jan. 2013.
- [4] A. Thiagarajan, K. Kaviarasan, R. Vigneshwaran, and K.M. Venkatraman, "The nano clay influence on mechanical properties of mixed glass fibre polymer composites," *Int. J. ChemTech Res.*, vol. 6, no. 3, pp. 1840-1843, March. 2014.
- [5] M.J. Kadhim, A.K. Abdullah, I.A. Al-Ajjaj, and A.S. Khalil, "Mechanical properties of epoxy/Al₂O₃ nanocomposites," *Int. J. Appl. Innov. Eng. Manage.*, vol. 2, no. 11, pp. 10-16, Nov. 2013.
- [6] A. Marcinčin, M. Hricová, A. Ujhelyiová, O. Brejka, P. Michlík, M. Dulíková, Z. Strecká, and Chmela, "Effect of inorganic (nano)fillers on the UV barrier properties, photo and thermal degradation of polypropylene fibres," *Fibres Text. East. Eur.*, vol. 17, no. 77, pp. 29-35, Jun. 2009.
- [7] W. Wang, and G. Huang, "Characterisation and utilization of natural coconut fibres composites," *Mater. Des.*, vol. 30, no. 7, pp. 2741-2744, Aug. 2009.
- [8] S. Husseinsyah, and M. Mostapha, "The effect of filler content on properties of coconut shell filled polyester composites," *Malay. Polym. J.*, vol. 6, no. 1, pp. 87-97, Jan. 2011.
- [9] V.O. Sousa Neto, T.V. Carvalho, S.B. Honorato, C.L. Gomes, F.C.F. Barros, M.A. Araujo-Silva, P.T.C. Freira, and R.F. Nascimento, "Coconut bagasse treated by thiourea/ammonia solution for cadmium removal: Kinetics and adsorption equilibrium," *BioResources*, vol. 7, no. 2, pp. 1504-1524, Jan. 2012.
- [10] P. Firoozian, I.U.H. Bhat, H.P.S. Abdul Khalil, Md.A. Noor, M.A. Hazizan, and A.H. Bhat, "High surface area activated carbon prepared from agricultural biomass: Empty fruit bunch (EFB), bamboo stem and coconut shells by chemical activation with H₃PO₄," *J. Eng. Mater. Technol.*, vol. 26, no. 5, pp. 222-228, Nov. 2011.
- [11] B.D. Reddy, S. Aruna Jyothy, and F. Shaik, "Experimental analysis of the use of coconut shell as coarse aggregate," *J. Mech. Civil Eng.*, vol. 10, no. 6, pp. 6-13, Jan. 2014.
- [12] W. Li, K. Yang, J. Peng, L. Zhang, S. Guo, and H. Xia, "Effects of carbonization temperatures on characteristics of porosity in coconut shell chars and activated carbons derived from carbonized coconut shell chars," *Ind. Crops. Prod.*, vol. 28, no. 2, pp. 190-198, Sep. 2008.
- [13] W. Su, L. Zhou, and Y.P. Zhou, "Preparation of microporous activated carbon from coconut shells without activating agents," *Carbon*, vol. 41, no. 2, pp. 861-863, Dec. 2003.
- [14] K.T. Paul, S.K. Satphaty, L. Manna, K.K. Chakraborty, and G.B. Nando, "Preparation and characterization of nano structured materials from fly ash: A waste from thermal power stations, by high energy ball milling," *Nanoscale Res. Lett.*, vol. 2, no. 8, pp. 397-404, Jul. 2007.
- [15] S. Ferreira-Dias, D.G. Valente, and J.M. Abreu, "Comparison between ethanol and hexane for oil extraction from Quercus suber L. fruits," *Grasas y Aceites*, vol. 54, no.4, pp. 378-383, Feb. 2003.
- [16] A.L. Patterson, "The Scherrer formula for X-ray particle size determination," *Phys. Rev.* vol. 56, no. 10, pp. 978-982, Nov. 1939.
- [17] H. Yang, R. Yan, T. Chin, D.T. Liang, H. Chen, and C. Zheng, "Thermogravimetric analysis-fourier transform infrared analysis of palm oil waste pyrolysis," *J. Energy. Fuels.*, vol. 18, no. 6, pp. 1814-1821, Oct. 2004.
- [18] J.H. Koo, "Polymer nanocomposites: processing, characterization, and applications. York New: McGraw-Hill, 2006, pp. 112-121.
- [19] S. Park, J.O. Baker, M.E. Himmel, P.A. Parilla, and D.K. Johnson, "Cellulose crystallinity index: measurement techniques and their impact on interpreting cellulose performance," *Biotechnol. Biofuels*, vol. 3, no. 10, pp. 1-10, May. 2010.
- [20] P.E. Imoisili, C.M. Ibegbulam, and T.I. Adejugbe, "Effect of Concentration of Coconut Shell Ash on the Tensile Properties of Epoxy Composites," *Pacific. J. Sci. Technol.*, vol. 13, no. 1, pp. 464-468, May. 2012.
- [21] J. Guo, and A.C. Lua, "Characterization of adsorbent prepared from oil-palm shell by CO₂ activation for removal of gaseous pollutant," *Mater. Lett.*, vol. 55, no. 5, pp. 334-339, Aug. 2002.
- [22] W.M.A.W. Daud, and W.S.W. Ali, "Comparison on pore development of activated carbon produced from palm shell and coconut shell," *Bioresour. Technol.*, vol. 93, no. 1, pp. 63-69, May. 2004.
- [23] K.V. Reddy, M. Das, and S.K. Das, "Filtration resistance in non-thermal sterilisation of green coconut water," *J. Food. Eng.*, vol. 69, no. 3, pp. 381-385, Aug. 2005.
- [24] Y.M. Afrouzi, A. Omidvar, and P. Marzbani, "Effect of artificial weathering on the wood impregnated with nano-zinc oxide," *World App. Sci. J.*, vol. 22, no. 9, pp. 1200-1203, Apr. 2013.
- [25] S. Fairus, S. Haryono, M.H. Sugita, and A. Sudrajat, A, "Waterglass making process of sand silica with natrium hydroxide," *J. Tek. Kim. Indo.*, vol. 8, no. 2, pp. 56-62, May. 2009.